Phase development and mechanical response of low-level cement replacements with wood ash and washed wood ash

Nina M. Sigvardsen[a,*], Mette R. Geiker[b], Lisbeth M. Ottosen[a]

[a] *Department of Civil Engineering, Technical University of Denmark, Kgs. Lyngby, Denmark*

[b] *Department of Structural Engineering, Norwegian University of Science and Technology, Trondheim, Norway*

Abstract

A significant increase is seen worldwide in the amounts of wood ashes (WAs) produced by the heating and power industry. This study investigates the potential utilisation of two different WAs as low-level cement replacements, in an untreated and a washed version. Phase development and mechanical response were investigated. Results indicated ettringite formation mainly to contribute to the strength development until excessive formation. Indications of an optimum SO_3/C_3A ratio for mixtures with a low-level cement replacement with WA was between 0.4 and 0.5. Washed WA originating from grate combustion appeared to be most promising of the tested WAs in cement-based materials.

Keywords: Wood ash, low-level cement replacement, phase development, mechanical response, cement-based material.

1. Introduction

Cement production accounts for 8-9% of the total anthropogenic CO_2 emissions [1], and the percentage is increasing due to a growing need for cement in developing countries [2]. One

* Corresponding author.
E-mail address: nimasi@byg.dtu.dk (N.M. Sigvardsen).

Abbreviations (not standard): WA1: untreated wood ash no. 1, WA2: untreated wood ash no. 2, WA1-W: wood ash no. 1 exposed to a preliminary washing treatment, WA2-W: wood ash no. 2 exposed to a preliminary washing treatment.

way to decrease the associated CO_2 emissions from cement production is the use of blended cement where a part of the cement is substituted with other materials. The production of ash deriving from biomass, organic materials such as wood, is increasing due to a withdrawal of the traditional coal-fired power plants in Europe [3], substituting coal with biomass in the heating and power production [4]. Currently, approximately 10 million tonnes of biomass ash are produced annually worldwide alone from the electricity production, thus for heat-only production, additional quantities of biomass ash can be added to the quantities [4]. This leads to a series of potentially new types of materials which can be used as a partial cement substitution in blended cement. Such a potential new material could be wood ash (WA), originating from combustion of wood and wood products [5].

The performance of wood ash in mortar and concrete, studied in the literature [5–11], vary significantly depending on the physicochemical characteristics of the WA utilised, again depending on, e.g. the type of wood fuel and combustion process used for the energy production [12,13]. This is clearly seen, e.g. from compressive strength measurements of mortar samples with a partial cement replacement of cement with different WAs; Udoeyo et al. [11], Berra et al. [6], and Elinwa and Mahmood [10] all saw a decrease in the compressive strength with increasing replacement rates, while Rajamma et al. [14] and Ramos et al. [7] observed a maintained compressive strength for samples with 10 and 20% cement replacements compared to a reference sample. Further, the properties of a WA can be improved by different types of pre-treatments; Berra et al. [6] included a washing step, Doudart de la Grée et al. [15] included both a sieving and washing step, and Rosales et al. [16] included grinding, heating and removal of remnants of charred wood, all pre-treatments improving the compressive strength measurements of cement-based materials with WA as a partial cement replacement. Washing of the WA reduces the content of soluble salts (such as chlorides and sulfates) [15]. These promising results encourage further studies, including pre-treatments and following both the strength and the phase development over time, as the latter has not been included in any of the previous studies, in order to increase the knowledge on how pre-treatment of WA influences the two. Based on previous studies, only low-level replacements (10wt%) of cement with WA, have seen to be feasible based on the compressive strength. This study continues these investigations on low-level replacements in order to determine the effects on the compressive strength and phase development at low-level cement replacements with WA.

The objectives of this study are: (1) to determine the impact of sieving and washing treatment of the WAs on the physicochemical characteristics; (2) to investigate the impact of a low-level

cement replacement with WA on the mechanical response and phase development as a function of time; and (3) to determine the influence of sieving and washing treatments before utilisation of WA as a low-level cement replacement according to the strength and phase development.

In the presented study, two types of WA originating from different types of combustion but using the same type of biofuel were investigated. The two investigated WAs originate from combustion of wood chips. One originates from grate combustion, and the other from circulating fluidised bed combustion. Wood chips for the energy production are one of the most commonly used biomasses, and the use has increased in consumption over the last 20 years (841% increase in the consumption of wood chips for the energy production since 2000 [17]). According to a recently published report by representatives from Austria, Canada, Denmark, Germany, Italy and the Netherlands [4] grate combustion is predominately used for combustion of biomass, but circulating fluidised bed combustion is gaining ground in many of the countries. These types of plants, grate or circulating fluidised bed combustion, have the highest efficiency when solely biomass is used [18], and are the most common type of plants regarding combustion of biomass. This means that the two chosen WAs represent common types of WAs.

2. Materials and methods

2.1. Materials

The materials used for this study were Portland cement, Rapid Aalborg Cement from Aalborg Portland, Denmark (CEM I), inert quartz (Qz) [19], and two types of wood fly ash, sampled at Skærbækværket Biomass Power Plant, Denmark (WA1) and Värtaverket Combined Heat and Power Plant, Sweden (WA2). WA1 is a residue from grate combustion (600-1,000°C). WA2 is a residue from circulating fluidised bed combustion (760-930°C). The fuel used at both plants was a similar type of wood chips originating from whole trees, primary pine trees, including bark and needles [20]. After sampling, the WAs were stored in closed plastic buckets protected from moist, heat and light sources. The buckets were rotated by hand in order to increase the uniformity of the WA before smaller portions of WA for further treatment were sampled. The WA samples were divided into two portions. The WAs were dried at 50°C and sieved. The sieving removed the particles ≥ 250μm, which consisted only of larger remnants from charred wood. The larger remnants of charred wood accounted for approximately 25% of WA1 and < 2% of WA2 when received from the power plants. Smaller particles of charred wood, which

can be found in the fraction ≤ 250µm [15], are not removed. One portion of each WA was subjected to drying at 50°C and sieving to a particle size of ≤ 250µm (termed WA1 and WA2). The other portion was washed after drying and sieving (termed WA1-W and WA2-W). The washing procedure was as follows: 100 g ash was mixed with distilled water to a liquid-to-solid ratio (L/S) of 5 and shaken manually for 1 min [21]. After settling (app. 5 min.), the water was decanted. This procedure was repeated three times, the suspension was filtered (retention 12-15µm), and the ash was subsequently dried at 50°C.

2.2 Methods

2.2.1 WA characterisation

Selected characteristics of the WAs, CEM I and Qz, are given in Tab. 2. Loss on ignition (LoI) was measured at 950°C, according to EN 196-2 [22]. The element content was determined by X-ray fluorescence (XRF) spectrometry measured by the use of a SPECTRO Gmbh X-LAB 2000 with a Pd-tube on samples ground to a particle size of less than 200µm. The software used was TQ-3945r, and the equivalent content of oxides was calculated based on the element content. Cl^- and SO_4^{-2} were measured with Ion Chromatography (IC) on a 1:2.5 solid-to-liquid ratio suspension in distilled water after 1 hour of agitation. The free calcium oxide contents in the WAs were measured according to EN 451-1 [23].

The particle size distribution was found by laser diffraction by the use of Mastersizer 2000. The pH was measured for all materials in 1:2.5 solid-to-liquid ratio suspensions in distilled water with a pH electrode after 1-hour agitation. The electric conductivity was determined on the same suspension with an electrical conductivity meter. The particle density was measured by the use of a helium gas pycnometer Micrometics AccuPyc 1340 in accordance with EN 196-6 [24].

The crystalline phases in the materials were identified by XRD. The WA was loaded into the sample holder using backloading. A PanAnalytical X-ray diffractometer, sat at the PW3064 Spinner stage for standard powder samples have been used for the measurements. Cu-Kα radiation with a wavelength of 1.54 Å was used as the x-ray source. The samples were measured between 4 °2θ and 100 5 °2θ with a step size of 0.002 °2θ and a sampling time per step of 24.8 s. The XRD plots were qualitatively evaluated using X'Pert HighScore Plus software, with data from the International Centre for Diffraction Data (ICDD). A semiquantitative analysis has been performed in X'Pert HighScore Plus software, determining

approximate amounts (in %) of the crystalline phases. The detection limited of the XRD analysis is 2 wt%. Grain morphology was analysed by the use of Scanning Electron Microscope (SEM)-images performed on a FEI Quanta 200. The pictures were magnified X1500, and the accelerating voltage of the beam was 20 keV with a large field detector under low vacuum conditions.

The thermogravimetric analysis (TGA) was performed on both WAs and WA-Ws. Approximate 40 mg of the sample was poured into 85 µl aluminium oxide crucibles (diameter 6.8mm), and the weight loss was measured from room temperature to 900 °C in a NETZSCH STA 449 F3 Jupiter. First, the temperature was raised to 40 °C and held for 10 min.; then the temperature was increased to 900 °C with a heating rate of 10 °C/min. During the measurements, the cell was purged with 50 ml/min of nitrogen gas. The data were processed using the analysis software Proteus Analyzer. The unburned carbon content was determined from LoI and TGA measurements.

2.2.2. Paste preparation and double solvent exchange

Six paste mixes were prepared, one reference and with 10% replacements of cement either with one of the four WAs or Qz with a constant w/b = 0.5. The pastes were mixed using a high shear mixer (Whip Mix Power Mixer Model B). The mixing procedure was adapted from EN 196-1 [25]: mixing for 90 s, resting for 90 s, and mixing for 60 s. The pastes were cast in 5 ml polythene tubes (diameter 12 mm) and stored for one day in a temperature-controlled room (20°C, <80% RH). The pastes were demoulded and transferred into larger 25 ml vials (diameter 25 mm), subsequently filled with lime water (3 g calcium hydroxide/L distilled water [26]) and stored in a temperature-controlled room (20°C). The pastes were tested after 1, 3, 7, 14, 28, 90, 182 and 365 days of hydration.

Double solvent exchange was used for hydration stoppage [27]. Four 2 mm thick slices (diameter 12 mm) were cut from the middle of the cured paste samples. The slices were crushed in a porcelain mortar until the whole paste sample could pass through a 1 mm sieve. Approximately 3g of the crushed sample was immersed in 50 mL isopropanol. The suspension was shaken for 30 sec, left to rest for 5 min, and subsequently decanted. This isopropanol treatment was performed twice, and then the suspension was vacuum-filtered. The crushed sample was then immersed in 10 mL diethyl ether, shaken for 30 sec, left to rest for 5 min., and vacuum-filtered [27]. The crushed cement paste (< 1mm) sample was shortly subjected to an

oven drying process (8 min. at 40°C) in order to remove the easily volatile diethyl ether. This method does not alter the hydrate products significantly [27]. For the TGA and XRD analysis, the paste samples were further crushed in a porcelain mortar, right before test execution, until the whole paste sample could pass through a 63µm sieve [27].

2.2.3. Thermogravimetric analysis (TGA)

Thermogravimetric analysis (TGA) was performed on pastes subsequently to the double solvent exchange treatment, drying and crushing. The TGA was performed as described in section 2.2.1. From the TGA measurements, the loss of bound water and decomposition of ettringite and calcite were determined by the use of a horizontal step and decomposition of portlandite was determined by the use of a tangential step. The step for bound water was 50°C and 550°C [27], for ettringite 50°C and 120°C [28], for portlandite 400°C and 550°C [27], and for calcite 550-800°C [27], respectively. It should be noted that the temperature interval for ettringite also includes carbonate AFm phases and C-S-H [28]. However, the included mass loss due to carbonate AFm phases was expected to be very small as the main peak of the carbonate AFm phases was determined to be above 120°C (approximately 160°C) as displayed in Fig. 5. The mass loss due to decomposition of C-S-H cannot be separated from the mass loss corresponding to ettringite as the TGA peaks overlap. This might lead to an overestimation of the amount of ettringite formed. However, this is acceptable as the WAs are not expected to contribute significantly to the formation of C-S-H compared to the formation of ettringite [29] due to a low content of silica in the WA, and the increase due to C-S-H can therefore mainly be attributed to the cement hydration. The equations for the quantification of the bound water (H), portlandite (CH), ettringite ($C_6As_3H_{32}$) and calcite ($C\overline{C}$) relative to the dry mass or clinker content (c.f. [27]) are given in Eqs. (1)-(12).

$$H_{measured} = WL_{50-550} \tag{1}$$

$$H_{anhydrous} = \frac{H_{measured}}{weight\ at\ 550°C} \tag{2}$$

$$H_{Clinker} = \frac{H_{measured}}{weight\ at\ 550°C} \times \frac{100}{\%clinker} \tag{3}$$

$$CH_{measured} = WL_{400-550} \cdot (74/18) \tag{4}$$

$$CH_{anhydrous} = \frac{CH_{measured}}{weight\ at\ 550°C} \tag{5}$$

$$CH_{Clinker} = \frac{CH_{measured}}{weight\ at\ 550°C} \times \frac{100}{\%clinker} \tag{6}$$

$$C_6As_3H_{32_{measured}} = WL_{50-120} \cdot (1255/(32 \cdot 18)) \quad (7)$$

$$C_6As_3H_{32_{anhydrous}} = \frac{C_6As_3H_{32_{measured}}}{weight\ at\ 550°C} \quad (8)$$

174

$$C_6As_3H_{32_{clinker}} = \frac{C_6As_3H_{32_{measured}}}{weight\ at\ 550°C} \times \frac{100}{\%clinker} \quad (9)$$

$$C\overline{C}_{measured} = WL_{550-800} \cdot (100/44) \quad (10)$$

$$C\overline{C}_{anhydrous} = \frac{C\overline{C}_{measured}}{weight\ at\ 550°C} \quad (11)$$

175

$$C\overline{C}_{Clinker} = \frac{CaCO_{3_{measured}}}{weight\ at\ 550°C} \times \frac{100}{\%clinker} \quad (12)$$

176 The standard deviations of these quantifications were based on three independent
177 measurements and quantifications of the bound water (H), portlandite (CH), ettringite
178 ($C_6As_3H_{32}$) and calcite ($C\overline{C}$) of a control sample at 28 days of hydration.

179 *2.2.4. X-ray diffraction (XRD)*

180 X-ray diffraction (XRD) analysis was performed on the same pastes used for the TGA
181 subsequently to the double solvent exchange treatment, drying and crushing. The XRD analysis
182 was performed, as described in section 2.2.1. Semiquantitative analysis was performed in
183 X'Pert HighScore Plus software, determining approximate amounts (in %) of the crystalline
184 phases.

185 *2.2.5. Preparation of mortar samples and compressive strength testing*

186 Mortar mixes were prepared according to the mixing procedure prescribed in EN 196-1 [25]
187 with a constant w/b = 0.5. One control mix without WA (REF), five mixes with 10%, and five
188 mixes with 20% replacements of cement (in accordance with ASTM C311/C311M-13 [30]),
189 either with one of the four WAs or Qz. WA or Qz was added to the unhydrated cement before
190 mixing. Super plasticiser (Dynamon XTend from Mapei) was added to the mixing water and
191 in order to achieve standard consistency, thus keeping a constant w/b ratio. The consistency
192 was determined by flow table according to EN 1015-3 [31] for mixes containing WA or Qz,
193 see Tab. 1. Mortar prisms (40 x 40 x 160 mm) were cast in accordance with EN 196-1 [25].
194 Three mortar prisms were prepared for each of the mixes for each of the hydration ages. After
195 1 day in a temperature-controlled room (20°C, <80% RH) the three prisms from each mix were
196 demoulded and stored in separate boxes submerged in lime water (3 g calcium hydroxide/L

distilled water [26]) in a temperature-controlled room (20°C). The mortar specimens with 10% replacements were tested after 1, 3, 7, 14, 28, 90, 182 and 365 days of hydration and the mortar specimens with 20% replacements were tested after 7 and 28 days of hydration [32].

After hydration, the compressive strength of the mortar specimens was determined according to EN 196-1 [25]. The mortars were split in two with an electro-mechanic test machine (Instron 6022) by increasing the load by 0.05 kN/s [25], and the compressive strength was measured for all the subsequent six pieces of mortar with a servohydraulic test machine (Toni Technik 300Ton) by increasing the load by 2.4 kN/s [25]. The air content of mortars was determined in accordance with Osbæck [33] by the use of the weight at demoulding and the theoretical air void free mortar. The compressive strength was then normalised to an air content of 2 vol% by the use of Bolomeys equation [34]. SAI was calculated according to ASTM C311/C311M-13 [30].

3. Results

3.1 Characteristics of WAs and Qz

DTG curves for all materials are displayed in Fig. 1. Some prehydration of CaO resulting in portlandite formation were seen for the washes ashes as a result of the washing treatment. The chemical composition of the materials is presented in Tab. 2 and the physical properties are presented in Tab. 3. A total below detection limit of Cl^- and SO_4^{2-} and a reduction in the content of alkali metals K_2O and Na_2O are results from the washing of WAs. Tab. 4 displays the crystalline phases for the materials and hydration of CaO to $Ca(OH)_2$ is seen for washed WAs. The grain morphology is shown by SEM images (Fig. 3). This reveals large, angular particles for both WAs. A layer of soluble compounds covers the untreated WAs, Fig. 3 (a) and (c), seen as minor particles covering larger particles. When the WAs were washed, Fig. 3. (b) and (d), this layer was removed. More spherical particles were found in WA1-W compared to WA2-W. The washing did not improve LoI of the WAs, which are high ($\geq$ 15%) for all WAs. The unburned carbon content was $\leq$ 1% for both WA1 and WA1-W and 6 and 7% for WA2 and WA2-W respectively.

3.2. Strength activity index

For pozzolanic activity, the ASTM C618 [32] requires an SAI above 0.75 compared to the reference after 7 and 28 days of hydration for a mortar sample containing 20% possible pozzolan and 80% CEM I as binder. The SAI are presented in Tab. 5 and only WA1 mortar does not comply with the limit. The washing treatment leads to an increase in the SAI for both types of WAs. Qz also complies with the limit, even though it being completely inert.

3.3. Compressive strength development

At 1 day of hydration, the compressive strength of the WA1 mortar is comparable to REF, see Fig. 4 and Tab. 6. The rest of the WA mortars obtains a slightly lower compressive strength, and a tendency is seen, where the washed WA mortars are more comparable with the Qz mortar. At 3 days the compressive strength for all WA mortars is comparable to REF and higher than the Qz mortar. From 7 days of hydration, the compressive strength of REF exceeds all WA and Qz mortars. At 90 ≤ days of hydration, all WA mortars have a slightly higher compressive strength compared to the Qz mortar. The WA1-W mortar exceeds the compressive strength of all other WA mortars, followed by, in decreasing order, the WA2, WA1 and WA2-W mortar.

3.4. Phase development

The phase development was analysed by XRD and TGA. Tab. 7 is an overview of the detected phases in the pastes determined by XRD. Depletion of alite was seen after 3 days of hydration for all pastes. Depletion of belite and ferrite are seen after 14 days of hydration for WA1-W and Qz paste, and for the remaining pastes after 28 days of hydration. Portlandite and ettringite were detected in all pastes from 1 days of hydaration and monocarbonate was detected in all pastes from 14 ≤ days of hydration. Quartz is detected in WA, and Qz pastes, at all hydration ages. Calcite is detected at 1 day of hydration for all WA pastes. However, dissolution of the calcite is seen for WA2 and WA2-W pastes since no calcite is detected again before 90 days of hydration.

Differential thermogravimetric (DTG) curves, determined with TGA for all pastes at 28 days of hydration, are presented in Fig. 5. The DTG curves show peaks of weight changes related to the decomposition of ettringite (Et) and C-S-H, monocarbonate (Mc) and portlandite (CH). Above 550°C, calcite decomposes by emitting CO_2 [27], substantiating the change from hydration to carbonation to be at 550°C as used in the formulas (1) – (12).

Quantification of bound water, portlandite, ettringite/C-S-H and calcite in all pastes are presented in Fig. 6, 7, 8 and 9, (a) calculated as wt%/anhydrous binder weight and (b) calculated as wt%/clinker content. The standard deviation was 0.67%wt for the quantification of bound water, 0.56%wt for the quantification of portlandite, 0.27%wt for the quantification of ettringite and 0.33%wt for the quantification of calcite. This is illustrated as error bars in the figures 6-9.

3.4.1. Bound water

At 1-3 days of hydration, a slightly larger amount of water was bound in the WA pastes compared to REF, see Fig. 6 (a)). After 7 days of hydration, the amount of bound water in REF and WA pastes were comparable. At 14 and 28 days of hydration, the amount of water bound in REF slightly exceeds the amount bound in the WA pastes. At 365 days the amount of bound water in REF and WA pastes are in the same range, but with a slightly higher amount of bound water in WA2 and WA2-W pastes compared to WA1 and WA1-W pastes. Qz had the lowest content of bound water of all pastes.

3.4.2. Portlandite

At 1-3 days of hydration, the portlandite content in WA and Qz pastes is similar or slightly higher than REF (Fig. 7 (a)). At 7 days, the portlandite content for REF paste increases compared to WA and Qz pastes, which remains comparable for the rest of the hydration period.

3.4.3. Ettringite

Ettringite has been determined for both REF and WA pastes at all ages (Tab. 7). A comparable ettringite content (Fig. 8 (a)) is seen for WA pastes from 1 to 7 days of hydration. From 14 ≤ days of hydration, the ettringite content in the WA pastes exceeds REF. This is especially notable for WA2 paste from 90 days of hydration and, at later ages (182 ≤ days of hydration), the same is seen for WA1 paste. Qz had the lowest content of ettringite at all ages.

3.4.4. Calcite

A clear difference is seen in the calcite content between WA1 and WA1-W pastes, and WA2 and WA2-W pastes at all ages (Fig. 9 (a)), with WA1 and WA1-W pastes having the highest content of calcite. The calcite content decreased from 1-90 days of hydration for all pastes followed by an increase after 90 days.

3.4.5. Dilution effect

In the pastes, the most reactive part (the cement) is replaced with a less or non-reactive material (WA or Qz). In order to take this dilution effect into account when analysing the results, the amount of bound water, portlandite, ettringite and calcite are calculated as wt%/clinker content, see Fig. 6, 7, 8 and 9 (b). The WA pastes have a higher amount of bound water than REF, and Qz pastes at all ages, see Fig. 6 (b). From 28 days of hydration, a slight increase in the portlandite content is seen for REF compared to WA and Qz pastes (Fig. 7 (b)). For the ettringite (Fig. 8 (b)) and calcite content (Fig. 9 (b)), Qz exceeds the contents calculated for REF.

4. Discussion

In the following section, the objectives 1-3 outlined in section 1 will be discussed based on the results presented in section 3.

4.1. Impact of the washing on the physicochemical characteristics of the WAs

Washing of the WAs resulted in a slight increase of the particle size distribution (Fig. 2) by removing the soluble fraction consisting of compounds with smaller particle sizes. This is supported by the SEM images (Fig. 3). Fig. 3 (a) and (c) reveals a layer of smaller compounds covering the particles of the raw WAs. These compounds are removed by washing, see Fig. 3. (b) and (d), and are thus assumed soluble, probably salts with Cl^- and SO_4^{2-} and the alkali metals, K and Na such as KCl, K_2SO_4 (Tab. 4) and NaCl, Na_2SO_4, as these chemical elements are removed to below detection limit or significantly reduced (Tab. 2). No decrease of neither LoI nor the unburned carbon content is seen as a result of the washing. The sieving effectively removed unburned carbon from WA1 and WA1-W, however, smaller particles ($\geq 250\mu m$) of unburned carbon are found in WA2 and WA2-W, containing 6 and 7% unburned carbon, respectively. The unburned carbon can lead to an increase in the water requirement [12,35,36]. However, this was not seen for the WAs investigated in this study. The high LoI measured for all WAs are primarily due to the content of hydrate phases and especially carbonate phases and not a high content of unburned carbon. The content of free CaO is decreased by the washing, however, it could still present an issue regarding soundness of the blended cement.

Several other issues are possible when utilising these WAs as a partial cement replacement, e.g. P_2O_5 can cause delayed set, alkalis can cause alkali silica reactions and SO_3 can cause sulfate attack. In relation to the durability, washing improves the possible use of WAs as a partial cement replacement, but further treatments will possibly be required before utilisation in cement-based materials is possible. However, as these issues are not investigated in this study, this needs to be addressed further in a subsequent study.

The washing further caused a difference in the phase composition of the WAs. From the DTG curves (Fig. 1) of the unhydrated materials, C-S-H (as no ettringite was determined by XRD) and an increase in the calcite content can be found in the washed WAs. The increase in calcite is substantiated by the XRD (Tab. 4.) and is due to removal of other water-soluble compounds and carbonation. Portlandite has been determined for all WAs by the XRD (Tab. 4.), but the DTG curves (Fig. 1) reveals a difference in the impact of the washing on the Portlandite content between the two types of WAs. The content of portlandite increases after the washing of WA1, but decreases for WA2. For both washed WAs, a chemical prehydration process between CaO and the content of water forming portlandite following reaction (13) is expected [29], as no CaO are found in the washed WAs (Tab. 4.) and a significant reduction is seen in the content of free CaO (Tab. 2) are seen. Subsequently, carbonation occurs in WA2-W, decreasing the content of portlandite and leading to calcite formation, following reaction (14) [37–39].

$$CaO + H_2O \rightarrow Ca(OH)_2 \quad (13)$$

$$Ca(OH)_2 + CO_2 \rightarrow CaCO_3 + H_2O \quad (14)$$

The initial content of portlandite and calcite in the untreated ashes are a consequence of water and CO_2 in the air during ash storage at the power plants, following reactions (13) and (14).

Arcanite (K_2SO_4) was determined in WA1 by XRD WA1, see Tab. 4. Formation of arcanite in the ash is due to a higher release of alkali metals by volatilisation facilitated by the high temperatures in grate combustion, compared to a fluidised bed system [40]. Arcanite is water-soluble and is removed during the washing, and thus it is not present in WA1-W (Tab. 4).

Sylvite (KCl) and anhydrite ($Ca(SO_4)$) were identified in WA2 by XRD, see Tab. 4. Thus, in WA2 potassium is primarily bound with chloride rather than sulfate, and sulfate is bound primarily to calcium. Anhydratie is a result of a sulphation process at the power plant were limestone are added to capture SO_2, an important process in a fluidised bed system,

precipitating anhydrite [40]. Neither sylvite nor anhydrite is present in WA2-W (Tab. 4) because these compounds are water-soluble, and the lime present in WA2 is hydrated to portlandite following reaction (13).

The initial presence of calcite has a beneficial impact on the properties of a cementitious material due to the potential formation of hemi- and monocarbonate. These AFm phases are more stable than monosulfate in the presence of carbonates [41], and as a consequence, ettringite does not transform into monosulfate, but is stabilised. Stabilisation of ettringite leads to an increase in compressive strength, as ettringite has a lager content of hydrate water and is more voluminous, leading to a reduction in the porosity [29,42–44]. Reactions (13) and (14) can occur during hydration of cement paste with partial cement replacement with WA due to hydration of CaO and subsequently carbonation [39], as CaO is present in both WA1 and WA2 and $Ca(OH)_2$ is present in all WAs (Tab. 4.).

4.2. Impact of the partial cement replacement of cement with WA on SAI, mechanical response and phase development

4.2.1. Strength activity index

From the results from the SAI test (Tab. 5), WA1-W, WA2 and WA2-W are seen to possess pozzolanic properties, meeting the requirements set by ASTM C618 [32] at both 7 and 28 days of hydration. A decrease of 20% and 15% decrease in the strength compared to REF are seen for Qz at 7 and 28 days of hydration, respectively, thus Qz complies with the requirements set by ASTM C618 [32]. However, Qz is completely inert and does not contribute through either nucleation processes or particle packing, due to the large particle size of Qz comparted to CEM I (Fig. 2) [45].

The SAI test an indirect method measuring a physical property indicating the extent of pozzolanic activity of a material [46]. According to the literature [47–49], there are several drawbacks of this method. An unreactive material can be misread as having pozzolanic properties, e.g. due to nucleation processes and particle packing effects [50,51] and other hydrate phases contributing to the compressive strength cannot be distinguished from the hydrate phases resulting from pozzolanic activity. Further ASTM C618 [32] requires measurements only at 7 and 28 days of hydration, which for some types of pozzolans is

inadequate, e.g. coal fly ash shows very little pozzolanic reactivity 28 days of hydration [38]. Amorphous silica and aluminosilicate leads to pozzolanic activity [52]. Due to the WAs consisting of large and fibrous particles (Fig. 3) and not the typical glassy aluminosilicate spherical particles found in commercial coal fly ash [53], the amount of amorphous glass are considered to be limited in the WAs. Further, the content of silica in WA1 and WA1-W are low (< 13%), see Tab. 2. The silica content in WA2 and WA-2-W is higher (23.8 and 26.5%, respectively), but this can be attributed to inert sand particles, which make the suspension bed and are carried with the flue gas during combustion with the circulating fluidised bed technology ending up in the fly ash fraction [40]. Thus a very limited pozzolanic reaction with silica [43] can be expected and the increase in strength can mainly be due to the WAs contributing through hydration of other hydrate phases, like ettringite, contributing to an increase in compressive strength [42]. No contribution through heterogeneous nucleation processes from WAs are expected either due to their particle size distribution being equivalent or larger than CEM I, see Fig. 2 [45].

4.2.2. Mechanical response

The development of compressive strength, when WAs are used as a partial cement replacement, is seen in Fig. 4. At 1 day of hydration WA1 and WA2 mortars have compressive strength comparable to the compressive strength of REF, and higher compressive strength compared to the mortars with WA1-W, WA2-W and Qz. The compressive strength of the mortar with WA1 is comparable to REF at both 1 and 3 days of hydration. All mortars containing WA, has a slightly higher compressive strength than the mortar with Qz at 1-7 days of hydration.

No contribution through heterogeneous nucleation processes from the WAs are expected, as described in section 4.2.1, thus the increase in the compressive strength of WA mortars being comparable to REF and not Qz at yearly age indicates an influence from chemical reactions due to dissolution of easily soluble salts leading to strength improving hydration products [29,42–44].

At late age, 90 ≤ days of hydration, all WA mortars have a higher compressive strength than the Qz mortar. The low compressive strength of Qz is due to the inert nature of the Qz and a low density (2650kg/m^3 compared to 3180kg/m^3 for CEM I), resulting in a larger volume based

addition of Qz, leading to relatively less space available for the hydrate formation further decreasing the strength.

At 365 days of hydration the average compressive strength for mortar with WA1 arrives at 86%, WA2 at 87%, WA1-W at 91%, WA2-W at 84% and Qz at 82% compared to the compressive strength of REF. The lower compressive strength of WA mortars reflects the dilution effect, decreasing the amount of hydrated cement and the larger volume based addition of the WA compared to CEM I. However, the increase in compressive strength compared to Qz indicates that the WA mortars facilitates the development of phases contributing to an increase in the compressive strength.

4.2.3. Phase development

4.2.3.1. Bound water

An increase in the amount bound water is seen for WA pastes at 1-3 days of hydration (Fig. 6 (a)) compared to REF. Such increase can be explained by the dissolution of easily soluble salts enhancing the initial growth of hydrated phases. From 14 to 90 days of hydration, the bound water in REF exceeds all WA pastes, but at 365 days of hydration, all WA pastes have approximately the same amount of bound water as the REF, indicating a continuous hydration of phases in the WA pastes compared to REF. WA2 and WA2-W pastes contain a slightly higher amount of bound water compared to WA1 and WA1-W pastes. This is explained by WA2 and WA2-W binding more water in phases such as ettringite (see Fig. 8).

The amount of bound water for WA pastes exceeds Qz at all ages (Fig. 6 (a)). These observations correspond to the WAs contributing through a quick initial dissolution of the particles at early age and development of phases contributing to the compressive strength at later ages.

4.2.3.2. Portlandite

Initially (1-7 days), the content of portlandite for all pastes with WAs exceeds the content of portlandite for pastes with Qz (Fig. 7 (a)). The increase in portlandite, compared to Qz, can be explained by an additional formation of portlandite due to a reaction between CaO in the WAs and H_2O (Eq. 13).

After 28 days of hydration, the portlandite content in WA pastes is slightly exceeded by the portlandite content of Qz when the dilution effect is considered (Fig. 7 (b)). This is explained by consumption of portlandite in the WAs either as a result of, to a minor extent, the pozzolanic reaction or formation of ettringite occurring at the expense of portlandite, aluminium and sulfate [41].

4.2.3.3. Ettringite/C-S-H

As discussed previously (section 2.2.3.) the formation of C-S-H cannot be separated from the mass loss corresponding to ettringite as the TGA peaks overlap, thus ettringite discussed in this section can include C-S-H. Some initial C-S-H is determined for washed WAs, however, based on the discussions presented in section 4.2.1. and 4.2.2. the WAs are not expected to contribute significantly to the formation of C-S-H compared to the formation of ettringite, substantiated by the literature [29]. Further, ettringite has been determined for both REF and WA pastes by XRD at all ages (Tab. 7).

A difference is seen at 1 day of hydration for the ettringite content between pastes with untreated and washed WAs (Fig. 8), corresponding to the initial C-S-H content and not ettringite found in WA1-W and WA2-W (Fig. 1.) A rapid increase in the ettringite content is seen for WA1 and WA2 from 1 to 3 days of hydration, corresponding to the dissolution of SO_4^{2-} in the untreated ashes (Fig. 8.).

All WA pastes have a higher content of ettringite than Qz at all ages and REF from 28 days of hydration, see Fig. 8 (a). The increase mainly contributed to the ettringite formation in WA pastes is attributed to an increase in the SO_3/C_3A ratio [38] and not formation of C-S-H. The content of ettringite was highest in the paste with WA2, corresponding well to WA2 having the largest initial content of SO_3 (Tab. 2). WA1 has the second-largest initial content of SO_3 and the second-largest content of ettringite at 182 ≤ days of hydration. These tendencies are consistent with the increased amount of bound water (Fig. 6 (b)) in WA pastes. Due to the amount of hydrate water, ettringite is voluminous, which leads to a reduction in the porosity and consequently to an increase in compressive strength [29,42–44]. At 182 ≤ days of hydration, the washed WA pastes have a lower ettringite content, compared to the untreated WAs, due to a lower SO_3 content (Tab. 2).

There was no decrease in the ettringite content due to stabilisation as a result of the presence of calcite and formation of monocarbonate (determined by the TGA, Fig. 5, and XRD Tab. 7.).

462 *4.2.3.4. Calcite*

463 A significant difference in the content of calcite at 1 day of hydration is seen between pastes
464 with WA1 and WA1-W, WA2 and WA2-W, and Qz and REF, see Fig. 9 (a). This is due to a
465 difference in the initial content of the materials: calcite contribution from WA and 5 %
466 limestone filler in CEM I. WA1 and WA1-W pastes have approximately 2 wt% higher content
467 of calcite than WA2 and WA2-W pastes (Fig. 9 (a)), attributed to a higher initial content of
468 calcite in WA1 and WA1-W (Fig. 1).

469 A decrease in calcite content is seen for all pastes from 1-90 days of hydration, especially
470 profound for WA pastes, due to formation of mono- and hemicarbonate at the expense of calcite
471 (determined by the TGA, Fig. 5, and XRD Tab. 7.). An increase in the calcite content is seen
472 from 90 ≤ days of hydration (Fig. 9 (a) and (b)), due to carbonation at later ages for WA pastes.

473

474 *4.3. Impact of washing on phase and compressive strength development*

475 Several differences were seen between the two types of WAs, before and after washing when
476 utilised in as low cement-replacements in cement-based materials. More ettringite is found in
477 pastes with untreated WA, compared to pastes containing washed WA, due to a larger SO_3
478 content in untreated WAs. The washing leads to a higher content of calcite due to removal of
479 soluble and carbonation occurring during washing. In general, the contribution to the
480 compressive strength from the WAs is mainly due to the formation of ettringite as a result of
481 an increased SO_3/C_3A ratio and stabilisation by calcite forming monocarbonate [41]. However,
482 excessive formation of ettringite can lead to micro-cracking and a decrease in strength if the
483 stress exceeds the tensile strength of the binder [38]. This can explain the different results
484 obtained for WA mortars, where WA1-W obtains a compressive strength above 90% the
485 reference strength and the compressive strength of WA1, WA2 and WA2-W all arrive at
486 between 84-87%.

487 A sufficient amount of ettringite is precipitated in WA1-W in order to increase the strength,
488 but low enough not to facilitate micro-cracks. The content of C_3A in the clinker can be
489 calculated by the use of Bogue calculations based on the content of Al_2O_3 and Fe_2O_3 [41], and
490 the SO_3/C_3A ratios are calculated for the WAs: WA1 = 0.5, WA1-W = 0.4, WA2 = 0.5, and
491 WA2-W = 0.5. This indicates the optimum SO_3/C_3A ratio of a mixture with a partial cement

replacement with WA to be: $0.4 \leq$ optimum < 0.5. This provides an indication of a sufficient removal of the SO_3 from a WA by a washing treatment order to obtain a sufficient, but not excessive amount of ettringite contributing positively to the strength development. The washing removed 76% of the SO_3 from WA1 and only 39% of SO_3 from WA2, thus further treatment should be conducted for WA2-W indicating WA1-W to be more promising as a low-level partial cement replacement.

Again, it should be noted that washing improves the possible use of WAs as a partial cement replacement, but further treatments will possibly be required before utilisation in cement-based materials is possible, especially considering several possible durability issues.

5. Conclusion

Two wood ashes (WAs), originating from two different power plants using circulating fluidised bed combustion and grate combustion, respectively, were investigated in an untreated as well as washed version for the purpose of low cement replacements (10%) in cement-based materials. The time-dependent development of bound water, portlandite, ettringite(/C-S-H) and calcite were measured in cement pastes with 10% replacement with the WAs. In general, increased content of bound water, ettringite and calcite, and decreased content of portlandite were seen for all pastes with WA compared to the Portland cement reference.

If only the mechanical response is considered, the results indicate that the WAs contributes to a minor extent to the compressive strength through pozzolanic reactions and the main contribution to the compressive strength are determined to be the ettringite content. However, excessive formation of ettringite leads to micro-cracking and a decrease in strength. Thus, the optimal ettringite content, contributing to the strength and not to micro-cracking, are found based on the SO_3/C_3A ratio for mixtures with low-level cement replacement with WA between 0.4 and 0.5.

For the two WAs investigated in this study, washed WA originating from grate combustion appears to be more promising as a low-level cement replacement a cement-based material compared to both untreated and washed WA originating from circulating fluidised bed combustion based on the compressive strength development.

6. Acknowledgement

The reported work was supported by the Department of Civil Engineering at the Technical University of Denmark and Emineral A/S. Scholarships were granted by Danielsen's Foundation and Spirekassen. Värtaverket Combined Heat and Power Plant and Skærbæk Power Plant are acknowledged for supplying the investigated wood ashes.

References

[1] P.J.M. Monteiro, S.A. Miller, A. Horvath, Towards sustainable concrete, Nat. Mater. 16 (2017) 698–699. doi:10.1038/nmat4930.

[2] UN Environment, K.L. Scrivener, V.M. John, E.M. Gartner, Eco-efficient cements: Potential economically viable solutions for a low-CO2cement-based materials industry, Cem. Concr. Res. 114 (2018) 2–26.

[3] A. Neslen, The end of coal: EU energy companies pledge no new plants from 2020 (Accessed 16th of November, 2018), Guard. (2017). https://www.theguardian.com/environment/2017/apr/05/the-end-of-coal-eu-energy-companies-pledge-no-new-plants-from-2020.

[4] A.S. Frans Lamers, Marcel Cremers, Doris Matschegg, Christoph Schmidl, Kirsten Hannam, Paul Hazlett, Sebnem Madrali, Birgitte Primdal Dam, Roberta Roberto, Rob Mager, Kent Davidsson, Nicolai Bech, Hans-Joachim Feuerborn, Options for increased use of ash from biomass combustion and co-firing, IEA Bioenergy Task 32. (2018) 1–61.

[5] R. Siddique, Utilization of wood ash in concrete manufacturing, Resour. Conserv. Recycl. 67 (2012) 27–33.

[6] M. Berra, T. Mangialardi, A.E. Paolini, Reuse of woody biomass fly ash in cement-based materials, Constr. Build. Mater. 76 (2015) 286–296. doi:10.1016/j.conbuildmat.2014.11.052.

[7] T. Ramos, A.M. Matos, J. Sousa-Coutinho, Mortar with wood waste ash: Mechanical strength carbonation resistance and ASR expansion, Constr. Build. Mater. 49 (2013) 343–351.

[8] R. Rajamma, R.J. Ball, L.A.C. Tarelho, G.C. Allen, J.A. Labrincha, V.M. Ferreira, Characterisation and use of biomass fly ash in cement-based materials, J. Hazard. Mater. 172 (2009) 1049–1060.

[9] S. Chowdhury, A. Maniar, O.M. Suganya, Strength development in concrete with wood ash blended cement and use of soft computing models to predict strength parameters, J. Adv. Res. 6 (2015) 907–913.

[10] A.U. Elinwa, Y.A. Mahmood, Ash from timber waste as cement replacement material, Cem. Concr. Compos. 24 (2002) 219–222.

[11] F.F. Udoeyo, H. Inyang, D.T. Young, E.E. Oparadu, Potential of wood waste ash as an additive in concrete, J. Mater. Civ. Eng. 18 (2006) 605–611.

[12] C.B. Cheah, M. Ramli, The implementation of wood waste ash as a partial cement replacement material in the production of structural grade concrete and mortar: An overview, Resour. Conserv. Recycl. 55 (2011) 669–685.

[13] R. Siddique, Wood Ash, in: Waste Mater. By-Products Concr., Springer Berlin Heidelberg, Berlin, Heidelberg, 2008: pp. 303–322.

[14] R. Rajamma, R.J. Ball, L.A.C. Tarelho, G.C. Allen, J.A. Labrincha, V.M. Ferreira, Characterisation and use of biomass fly ash in cement-based materials, J. Hazard. Mater. 172 (2009) 1049–1060.

[15] G.C.H. Doudart de la Grée, M.V.A. Florea, A. Keulen, H.J.H. Brouwers, Contaminated biomass fly ashes - Characterization and treatment optimization for reuse as building materials, Waste Manag. 49 (2016) 96–109.

[16] J. Rosales, M. Cabrera, M.G. Beltrán, M. López, F. Agrela, Effects of treatments on biomass bottom ash applied to the manufacture of cement mortars, J. Clean. Prod. 154 (2017) 424–435. doi:10.1016/j.jclepro.2017.04.024.

[17] Danish Energy Agency, Energy Statistics 2018, 2018.

[18] R. Van Den Broek, A. Faaij, A. Van Wijk, Biomass combustion for power generation, Biomass and Bioenergy. 11 (1996) 271–281. doi:10.1016/0961-9534(96)00033-5.

[19] X. Li, R. Snellings, M. Antoni, N.M. Alderete, M. Ben Haha, S. Bishnoi, Ö. Cizer, M. Cyr, K. De Weerdt, Y. Dhandapani, J. Duchesne, J. Haufe, D. Hooton, M. Juenger, S. Kamali-Bernard, S. Kramar, M. Marroccoli, A.M. Joseph, A. Parashar, C. Patapy, J.L. Provis, S. Sabio, M. Santhanam, L. Steger, T. Sui, A. Telesca, A. Vollpracht, F. Vargas, B. Walkley, F. Winnefeld, G. Ye, M. Zajac, S. Zhang, K.L. Scrivener, Reactivity tests for supplementary cementitious materials: RILEM TC 267-TRM phase 1, Mater. Struct. Constr. 51 (2018).

[20] N.M. Sigvardsen, G.M. Kirkelund, P.E. Jensen, M.R. Geiker, L.M. Ottosen, Impact of production parameters on physiochemical characteristics of wood ash for possible utilisation in cement-based materials, Resour. Conserv. Recycl. 145 (2019) 230–240.

[21] G.M. Kirkelund, L.M. Ottosen, P.E. Jensen, P. Goltermann, Greenlandic waste incineration fly and bottom ash as secondary resource in mortar, Int. J. Sustain. Dev. Plan. 11 (2016) 719–728.

[22] EN 196, Method of testing cement - Part 2: Chemical analysis of cement, (2013).

[23] EN 451, Method of testing fly ash – Part 1 : Determination of free calcium oxide content, (2017).

[24] EN 196, Methods of testing cement – Part 6: Determination of fineness, (2018).

[25] EN 196, Method of testing cement - Part 1: Determination of strength, (2016).

[26] ASTM C511-19, Standard Specification for Mixing Rooms, Moist Cabinets, Moist Rooms, and Water Storage Tanks Used in the Testing of Hydraulic Cements and Concretes, Am. Soc. Test. Mater. (2019) 1–3.

[27] K. Scrivener, R. Snellings, B. Lothenbach, A Practical Guide to Microstructural Analysis of Cementitious Materials, CRC Press, 2017.

[28] L. Pelletier-Chaignat, F. Winnefeld, B. Lothenbach, C.J. Müller, Beneficial use of limestone filler with calcium sulphoaluminate cement, Constr. Build. Mater. 26 (2012) 619–627.

[29] M. Illikainen, P. Tanskanen, P. Kinnunen, M. Körkkö, O. Peltosaari, V. Wigren, J. Österbacka, B. Talling, J. Niinimäki, Reactivity and self-hardening of fly ash from the fluidized bed combustion of wood and peat, Fuel. 135 (2014) 69–75. doi:10.1016/j.fuel.2014.06.029.

[30] ASTM International C311/C311M-13, Standard Test Methods for Sampling and Testing Fly Ash or Natural Pozzolans for Use in Portland-Cement Concrete., (2007) 204–212.

[31] EN 1015, Methods of test for mortar for masonry - Part 3: Determination of consistence of fresh mortar (by flow table), (1999).

603 [32] ASTM International C618-15, Standard Specification for Coal Fly Ash and Raw or Calcined
604 Natural Pozzolan for Use in Concrete, (2015).

605 [33] B. Osbæck, The influence of air content by assessing the pozzolanic activity of fly ash by
606 strength testing, Cem. Concr. Res. 15 (1985) 53–64. doi:10.1016/0008-8846(85)90008-0.

607 [34] G.N. Munch-Petersen, Betonhåndbogen, Dansk Betonforening, 2013.

608 [35] I. Carević, M. Serdar, N. Štirmer, N. Ukrainczyk, Preliminary screening of wood biomass ashes
609 for partial resources replacements in cementitious materials, J. Clean. Prod. 229 (2019) 1045–
610 1064. doi:10.1016/j.jclepro.2019.04.321.

611 [36] R. Rajamma, L. Senff, M.J. Ribeiro, J.A. Labrincha, R.J. Ball, G.C. Allen, V.M. Ferreira,
612 Biomass fly ash effect on fresh and hardened state properties of cement based materials,
613 Compos. Part B Eng. 77 (2015) 1–9. doi:10.1016/j.compositesb.2015.03.019.

614 [37] B.M. Steenari, L.G. Karlsson, O. Lindqvist, Evaluation of the leaching characteristics of wood
615 ash and the influence of ash agglomeration, Biomass and Bioenergy. 16 (1999) 119–136.

616 [38] P. Barnes, J. Bensted, Structure and Performance of Cements, 2nd ed., Taylor & Francis, London
617 and New York, 2002.

618 [39] B.-M. Steenari, O. Lindqvist, Stabilisation of biofuel ashes for recycling to forest soil, Biomass
619 and Bioenergy. 13 (1997) 39–50.

620 [40] S. van Loo, J. Koppejan, The Handbook of Biomass Combustion and Co-firing, Taylor &
621 Francis Ltd, 2010.

622 [41] P. Hewlett, M. Liska, Lea's Chemistry of Cement and Concrete, 5th ed., Elsevier Science, 2019.

623 [42] T. Sebok, J. Simonik, K. Kulisek, The compressive strength of samples containing fly ash with
624 high content of calcium sulfate and calcium oxide, Cem. Concr. Res. 31 (2001) 1101–1107.

625 [43] H. Justnes, Performance of SCMs – Chemical and Physical Principles, in: 2nd Int. Conf. Sustain.
626 Build. Mater., 2019.

627 [44] J. Skibsted, R. Snellings, Reactivity of supplementary cementitious materials (SCMs) in cement
628 blends, Cem. Concr. Res. 124 (2019) 105799. doi:10.1016/j.cemconres.2019.105799.

629 [45] K.L. Scrivener, B. Lothenbach, N. De Belie, E. Gruyaert, J. Skibsted, R. Snellings, A.
630 Vollpracht, TC 238-SCM: hydration and microstructure of concrete with SCMs: State of the art
631 on methods to determine degree of reaction of SCMs, Mater. Struct. Constr. 48 (2015) 835–862.
632 doi:10.1617/s11527-015-0527-4.

633 [46] S. Donatello, M. Tyrer, C.R. Cheeseman, Comparison of test methods to assess pozzolanic
634 activity, Cem. Concr. Compos. 32 (2010) 121–127.

635 [47] S. Ramanathan, H. Moon, M. Croly, C. Chung, P. Suraneni, Predicting the degree of reaction of
636 supplementary cementitious materials in cementitious pastes using a pozzolanic test, Constr.
637 Build. Mater. 204 (2019) 621–630. doi:10.1016/j.conbuildmat.2019.01.173.

638 [48] S. Donatello, A. Freeman-Pask, M. Tyrer, C.R. Cheeseman, Effect of milling and acid washing
639 on the pozzolanic activity of incinerator sewage sludge ash, Cem. Concr. Compos. 32 (2010)
640 54–61. doi:10.1016/j.cemconcomp.2009.09.002.

641 [49] R. Kalina, S. Al-Shmaisani, R.D. Ferron, M.C.G. Juenger, False Positives in ASTM C618
642 Specifications for Natural Pozzolans, ACI Mater. J. 116 (2019) 165–172.

643 [50] E. Berodier, K. Scrivener, Understanding the filler effect on the nucleation and growth of C-S-
644 H, J. Am. Ceram. Soc. 97 (2014) 3764–3773. doi:10.1111/jace.13177.

645 [51] P. Lawrence, M. Cyr, E. Ringot, Mineral admixtures in mortars Effect of inert materials on short-

term hydration, Cem. Concr. Res. 33 (2003) 1939–1947.

[52] C.R. Shearer, The Productive Reuse of Coal, Biomass and the Productive Reuse of Coal, Biomass and Co-Fired Fly Ash, Georgia Institute of Technology, 2014.

[53] N.N.N. Yeboah, C.R. Shearer, S.E. Burns, K.E. Kurtis, Characterization of biomass and high carbon content coal ash for productive reuse applications, Fuel. 116 (2014) 438–447.

Table 1. Consistency measured by flow table. The value SP to obtain REF are calculated via linear interpolation of the measured flow values in order to obtain a flow value equal to the average flow value of REF.

	SP	Measure 1	Measure 2	Measure 3	Measure 4	Average	SP to obtain REF
	[g]	[mm]	[mm]	[mm]	[mm]	[mm]	[g]
REF no. 1	0	173.0	176.0	176.2	175.0	174.3	-
REF no. 2	0	167.0	175.6	175.5	176.2		
WA1 no. 1	0.5	148.8	146.2	146.9	144.8	146.7	
WA1 no. 2	1.0	183.8	184.6	177.1	178.7	181.0	1.2
WA1 no. 3	2.4	206.7	201.9	206.5	207.0	205.1	
WA1-W no. 1	0.6	148.8	148.1	143.0	152.3	147.8	
WA1-W no. 2	1.0	169.1	173.7	166.8	159.1	167.2	1.2
WA1-W no. 3	1.5	182.8	194.2	181.6	191.1	187.4	
WA2 no. 1	0.5	172.2	178.9	171.6	166.5	172.3	
WA2 no. 2	0.8	183.6	182.5	179.8	185.1	182.7	0.6
WA2 no. 3	1.0	184.9	189.0	177.4	181.0	183.1	
WA2-W no. 1	0.5	174.0	172.4	164.4	164.0	166.9	
WA2-W no. 2	0.8	175.4	164.2	159.8	173.5	168.2	0.8
WA2-W no. 3	1.0	185.2	181.9	184.6	182.4	183.5	

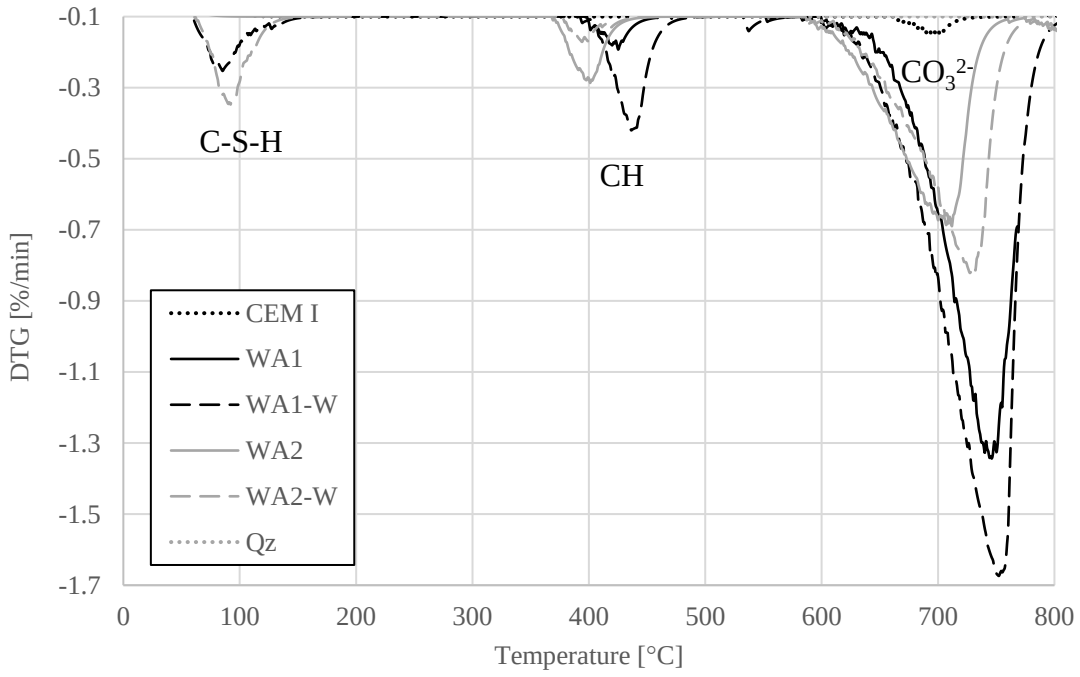

Figure 1. Differential thermosgravimetric (DTG) curves for unhydrated materials. C-S-H: Calium silicate hydrate, CH: Portlandite.

Table 2. Chemical composition (%) of CEM I, WA1, WA1-W, WA2, WA2-W, and Qz. ± defines the standard deviation. ND: not determined.

	CEM I	WA1	WA1-W	WA2	WA2-W	Qz
SiO_2	19.7	11.0	12.7	23.8	26.5	99.4
Al_2O_3	5.4	2.4	3.0	5.6	6.3	0.10
Fe_2O_3	3.8	2.9	3.2	3.1	3.3	0.03
CaO	64.1	53.6	65.0	44.7	45.0	0
MgO	1.0	4.2	5.8	4.1	4.4	0
K_2O	0.4	14.6	4.4	7.6	5.7	0
Na_2O	0.3	1.0	1.0	0.8	0.9	0
P_2O_5	0.3	2.9	3.8	3.8	4.2	0
SO_3	3.2	5.4	1.3	6.1	3.7	0
$CaO_{,\ free}$	ND	12.3	5.9	6.4	1.6	0
Cl^-	0.0 ± 0.0	0.8 ± 0.0	0.0 ± 0.0	0.4 ± 0.0	0.0 ± 0.0	0.0 ± 0.0
SO_4^{-2}	0.0 ± 0.0	3.8 ± 0.0	0.0 ± 0.0	1.8 ± 0.0	0.0 ± 0.0	0.0 ± 0.0
LoI, 950ºC	1.9 ± 0.0	15.0 ± 0.1	19.6 ± 0.1	16.2 ± 0.3	19.7 ± 0.1	0.0 ± 0.0
Unburned carbon	-	≥ 1.0	≥ 1.0	5.7	6.7	-

Table 3. Physical characteristics of CEM I, WA1, WA1-W, WA2, WA2-W, and Qz. ± defines the standard deviation.

	CEM I	WA1	WA1-W	WA2	WA2-W	Qz
pH	12.8 ± 0.0	13.0 ± 0.1	12.5 ± 0.0	12.7 ± 0.1	12.5 ± 0.2	7.7 ± 0.1
Conductivity (mS m^{-1})	18.1 ± 0.2	76.6 ± 0.4	11.1 ± 0.1	29.0 ± 1.3	11.9 ± 0.2	40.0 ± 2.5
Particle density (kg/m^3)	3180	2740	2640	2710	2650	2650

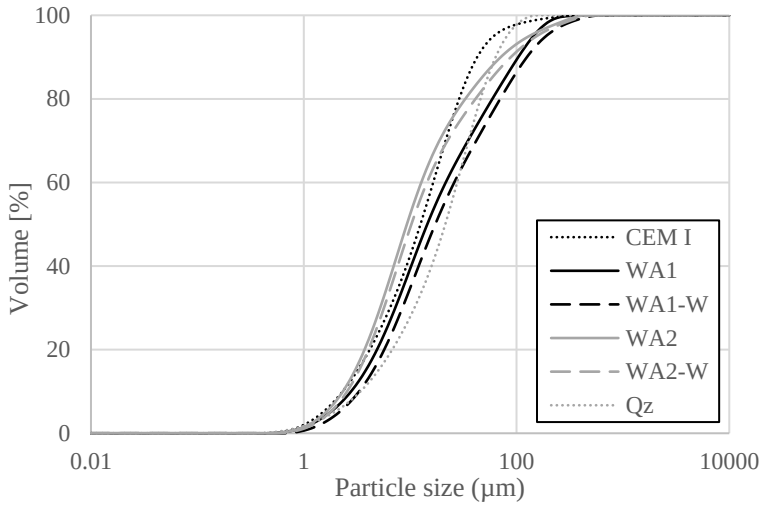

Figure 2. Particle size distribution of CEM I, WA1, WA1-W, WA2, WA2-W, and Qz, determined by laser diffraction.

Table 4. Crystalline phases for unhydrated materials determined qualitatively by XRD diffraction. x: < 15%, xx: ~ 25%, xxx: ~ 50% and xxxx: ~ 100% of crystalline phases identified according to semiquantitative analysis.

	Alite	Belite-β	C_3A	Ferrite	Portlandite	Lime	Quartz	Calcite	Sylvite	Arcanite	Anhydrite
CEM I	xxx	x	x	x							x
WA1					x	x	xx	xxx		x	
WA1-W					x		xx	xxx			
WA2					x	x	xxx	xx	x		x
WA2-W					x		xxx	xxx			
Qz							xxxx				

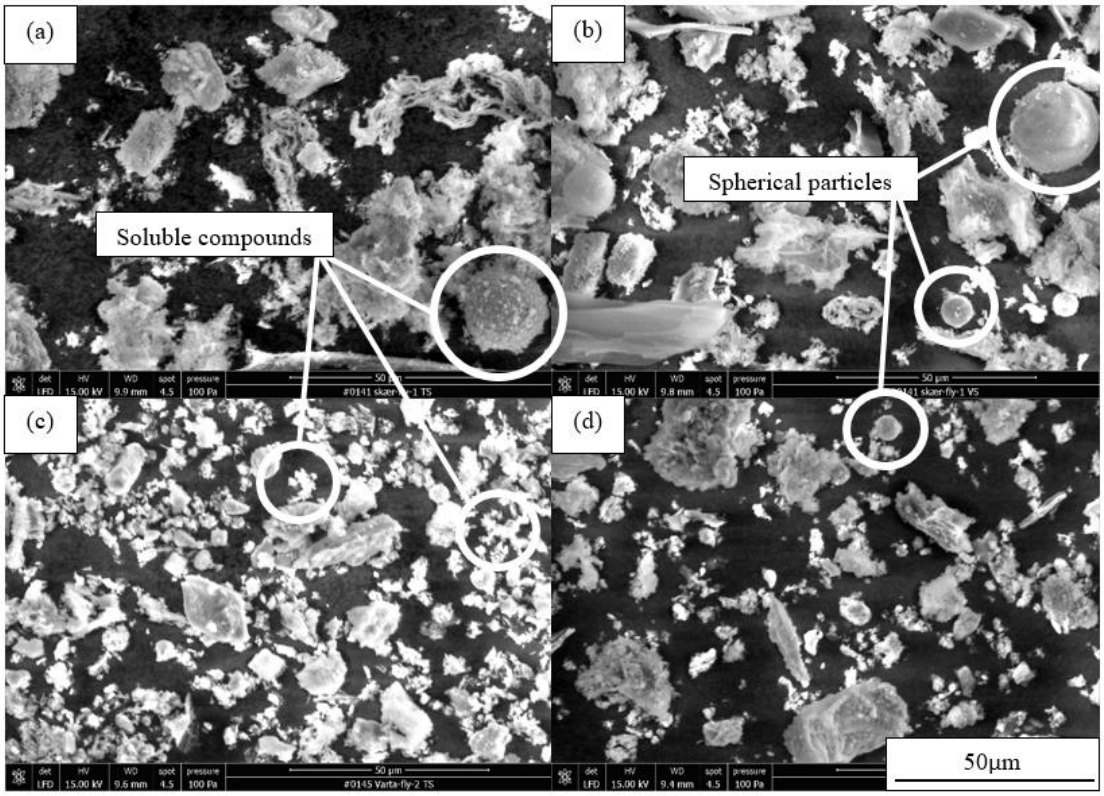

Figure 3. Grain morphology of (a) WA1, (b) WA1-W, (c) WA2 and (d) WA2-W.

Table 5. Measured compressive strength, air content, compressive strength normalised to an air content of 2 vol% by the use of Bolomeys equation [34] and SAI calculated according to ASTM C311/C311M-13 [30].

	Compressive strength (MPa)	SD	Air content (%vol)	Normalised compressive strength (MPa)	SAI
M7-REF	59.5	3.6	1.1	57.5	-
M7-20%WA1	44.1	0.7	1.0	42.6	0.74
M7-20%WA1-W	50.4	1.1	1.1	46.7	0.81
M7-20%WA2	50.3	0.7	1.0	48.7	0.85
M7-20%WA2-W	49.3	0.4	1.1	46.04	0.80
M7-20%Qz	45.9	0.9	1.0	44.1	0.77
M28-REF	69.9	1.8	1.1	64.7	-
M28-20%WA1	51.1	1.3	1.0	49.4	0.76
M28-20%WA1-W	59.3	2.7	1.1	55.0	0.85
M28-20%WA2	59.4	1.4	1.0	57.4	0.89
M28-20%WA2-W	57.0	0.7	1.1	53.24	0.82
M28-20%Qz	57.2	1.4	1.0	54.9	0.85

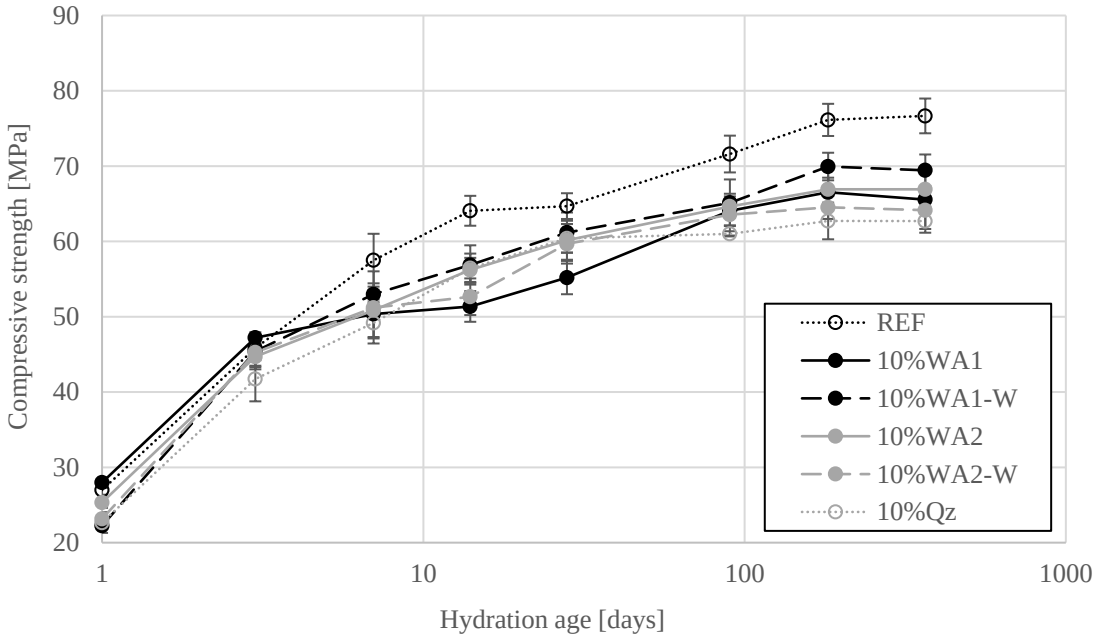

Figure 4. Development of compressive strength of REF and mortars with 10% replacements of cement with WA1, WA1-W, WA2, WA2-W, and Qz after 1, 3, 7, 14, 28, 90, 182 and 365 days of hydration at 20°C. The compressive strength normalised to an air content of 2 vol% by the use of Bolomeys equation [34]. The error bars defines the standard deviation.

Table 6. Measured compressive strength, air content and compressive strength normalised to an air content of 2 vol% by the use of Bolomeys equation [34].

	Compressive strength (MPa)	SD	Air content (%vol)	Normalised compressive strength (MPa)
M1-REF	27.9	0.6	1.1	27.0
M1-10%WA1	30.1	0.7	0.1	28.0
M1-10%WA1-W	23.2	1.0	0.9	22.3
M1-10%WA2	26.1	0.7	1.2	25.3
M1-10%WA2-W	24.8	0.9	0.2	23.2
M1-10%Qz	23.8	0.9	0.8	22.7
M3-REF	47.4	1.6	1.1	45.8
M3-10%WA1	50.8	0.8	0.1	47.2
M3-10%WA1-W	47.4	2.2	0.9	45.4
M3-10%WA2	46.1	1.7	1.2	44.7
M3-10%WA2-W	48.4	1.9	0.2	45.3
M3-10%Qz	43.8	3.1	0.8	41.7
M7-REF	59.5	3.6	1.1	57.5
M7-10%WA1	54.2	3.5	0.1	50.4
M7-10%WA1-W	55.3	3.2	0.9	53.0
M7-10%WA2	52.5	3.7	1.2	50.9
M7-10%WA2-W	54.8	1.2	0.2	51.2
M7-10%Qz	51.6	2.9	0.8	49.2
M14-REF	67.1	2.1	1.1	64.1
M14-10%WA1	55.3	2.2	0.1	51.4
M14-10%WA1-W	59.4	2.7	0.9	56.9
M14-10%WA2	58.0	1.6	1.2	56.2
M14-10%WA2-W	56.4	2.6	0.2	52.7
M14-10%Qz	59.2	2.0	0.8	56.4
M28-REF	69.9	1.8	1.1	64.7
M28-10%WA1	59.4	2.4	0.1	55.2
M28-10%WA1-W	63.9	2.8	0.9	61.2
M28-10%WA2	62.1	2.7	1.2	60.2
M28-10%WA2-W	63.9	2.8	0.2	59.7
M28-10%Qz	63.6	1.8	0.8	60.4
M90-REF	74.1	2.5	1.1	71.6
M90-10%WA1	68.9	2.1	0.1	64.1
M90-10%WA1-W	68.0	3.2	0.9	65.1
M90-10%WA2	66.7	1.1	1.2	64.6
M90-10%WA2-W	68.0	3.0	0.2	63.6
M90-10%Qz	64.0	0.4	0.8	61.0
M182-REF	78.8	2.2	1.1	76.1
M182-10%WA1	71.6	2.1	0.1	66.5
M182-10%WA1-W	73.0	1.9	0.9	69.9
M182-10%WA2	69.1	2.8	1.2	66.9
M182-10%WA2-W	69.1	1.7	0.2	64.5
M182-10%Qz	65.8	0.4	0.8	62.7
M365-REF	77.0	2.5	1.1	76.7
M365-10%WA1	70.5	1.4	0.1	65.6
M365-10%WA1-W	71.5	2.2	0.9	69.4
M365-10%WA2	69.1	2.4	1.2	66.9
M365-10%WA2-W	68.6	2.7	0.2	64.1
M365-10%Qz	67.9	1.6	0.8	62.7

Table 7. Crystalline phases for paste samples investigated after 1, 3, 7, 14, 28, 90, 182 and 365 days of hydration at 20°C determined qualitatively by XRD diffraction. x: < 15%, xx: ~ 25% and xxx: ~ 50% of crystalline phases identified according to semiquantitative analysis.

	Lime	Alite	Belite-β	Ferrite	Portlandite	Ettringite	Quartz	Calcite	Monocarbonate
P1-REF		xx	xx	x	xx	x			
P1-10%WA1	x	xx	xx	x	xx	x	x	x	
P1-10%WA1-W		xx	xx	x	xx	x	x	x	
P1-10%WA2	x	xx	xx	x	xx	x	x	x	
P1-10%WA2-W		xx	xx	x	xx	x	x	x	
P1-10%Qz		xx	x	x	x	x	xx		
P3-REF		xx	xx	x	xx	x			
P3-10%WA1		x	xx	x	xx	xx	x	x	
P3-10%WA1-W		xx	xx	x	xx	xx	x	x	
P3-10%WA2		x	xx	x	xxx	xx	x		
P3-10%WA2-W		x	xx	x	xx	xx	x		
P3-10%Qz		x	x	x	xx	xx	xx		
P7-REF			xx	x	xx	xx			
P7-10%WA1			xx	x	xx	xx	x	x	
P7-10%WA1-W			xx	x	xx	xx	x	x	
P7-10%WA2			x	x	xxx	xx	x		
P7-10%WA2-W			x	x	xx	xx	x		
P7-10%Qz			x	x	xx	xx	xx		
P14-REF			xx	x	xxx	xx			x
P14-10%WA1			x	x	xxx	xx	x	x	x
P14-10%WA1-W			x	x	xxx	xx	x	x	x
P14-10%WA2			x	x	xxx	xx	x		x
P14-10%WA2-W			x	x	xxx	xx	x		x
P14-10%Qz			x	x	xxx	xx	xx		x
P28-REF			x	x	xxx	xx			x
P28-10%WA1					xx	xx	x	x	x
P28-10%WA1-W			x	x	xx	xx	x	x	x
P28-10%WA2			x	x	xx	xx	x		x
P28-10%WA2-W			x	x	xx	xx	x		x
P28-10%Qz					xxx	xx	xx		x
P90-REF					xxx	xx			x
P90-10%WA1					xxx	xxx	x	x	x
P90-10%WA1-W					xxx	xx	x	x	x
P90-10%WA2					xxx	xx	x	x	x
P90-10%WA2-W					xxx	xx	x	x	x
P90-10%Qz					xxx	xx	xx		x
P182-REF					xxx	xx			x
P182-10%WA1					xxx	xxx	x	x	x
P182-10%WA1-W					xxx	xx	x	x	x
P182-10%WA2					xxx	xx	x	x	x
P182-10%WA2-W					xxx	xx	x	x	x
P182-10%Qz					xxx	xx	xx		x
P365-REF					xxx	xx			x
P365-10%WA1					xxx	xxx	x	x	x
P365-10%WA1-W					xxx	xx	x	x	x
P365-10%WA2					xxx	xxx	x	x	x
P365-10%WA2-W					xxx	xx	x	x	x
P365-10%Qz					xxx	xx	xx		x

701
702

703

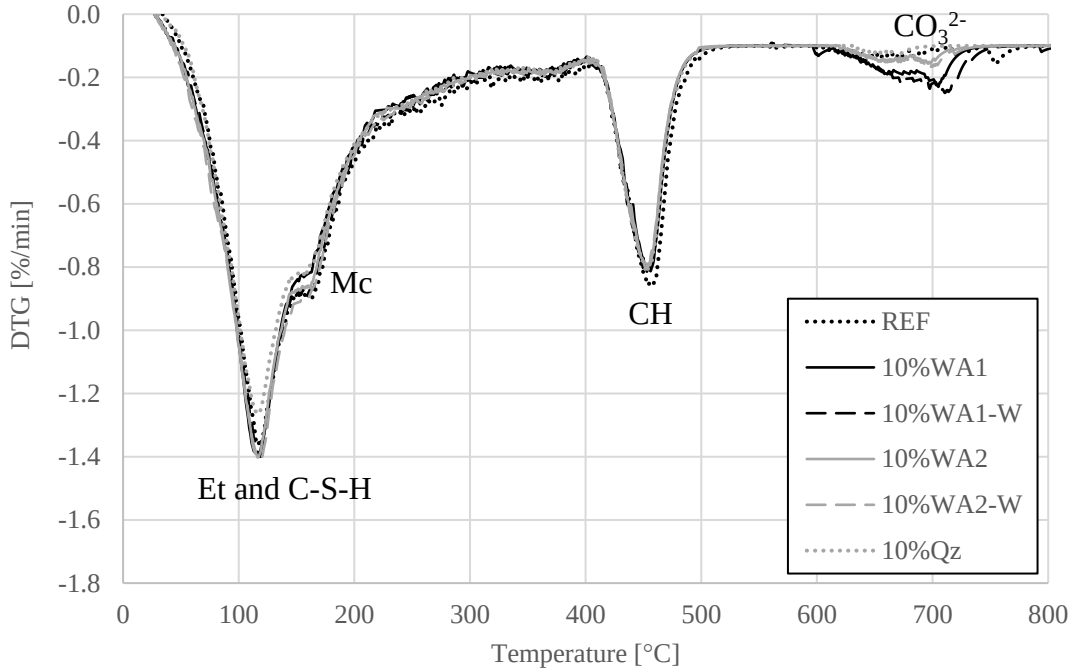

704 **Figure 5.** Differential thermosgravimetric (DTG) curves for paste samples investigated at 20°C after 28 days of
705 hydration. Et: Ettringite, C-S-H: Calium silicate hydrate, Mc: Monocarbonate, CH: Portlandite.
706

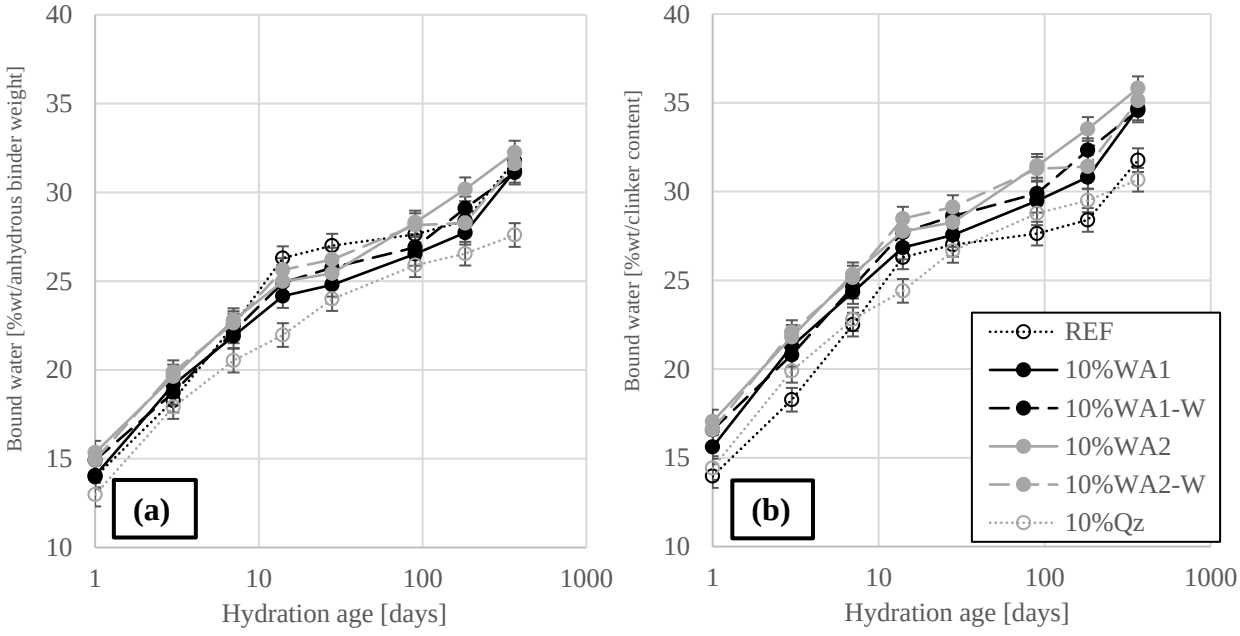

707

708
709 **Figure 6.** Quantification of bound water in paste samples investigated after 1, 3, 7, 14, 28, 90, 182 and 365 days
710 of hydration at 20°C. The results are normalised to the anhydrous binder (a) and clinker content (b). Standard
711 deviations are based on three independent measurements and quantifications of the bound water of a control
712 sample at 28 days of hydration.

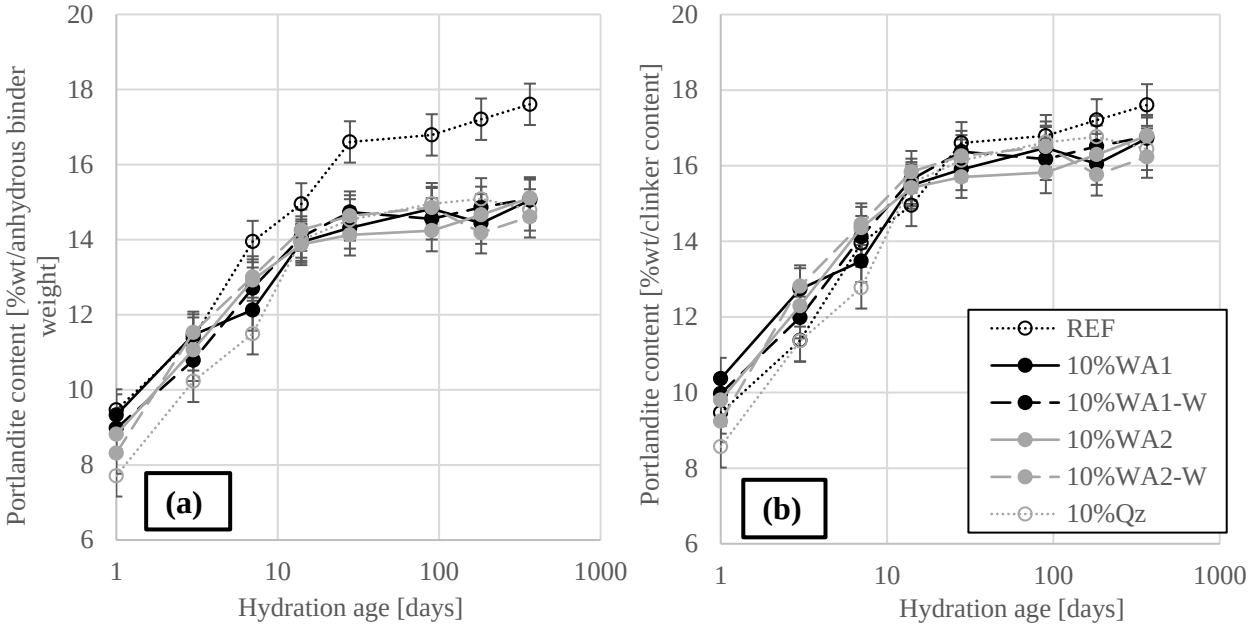

Figure 7. Quantification of portlandite in paste samples investigated after 1, 3, 7, 14, 28, 90, 182 and 365 days of hydration at 20°C. The results are normalised to the anhydrous binder (a) and clinker content (b). Standard deviations are based on three independent measurements and quantifications of the portlandite of a control sample at 28 days of hydration.

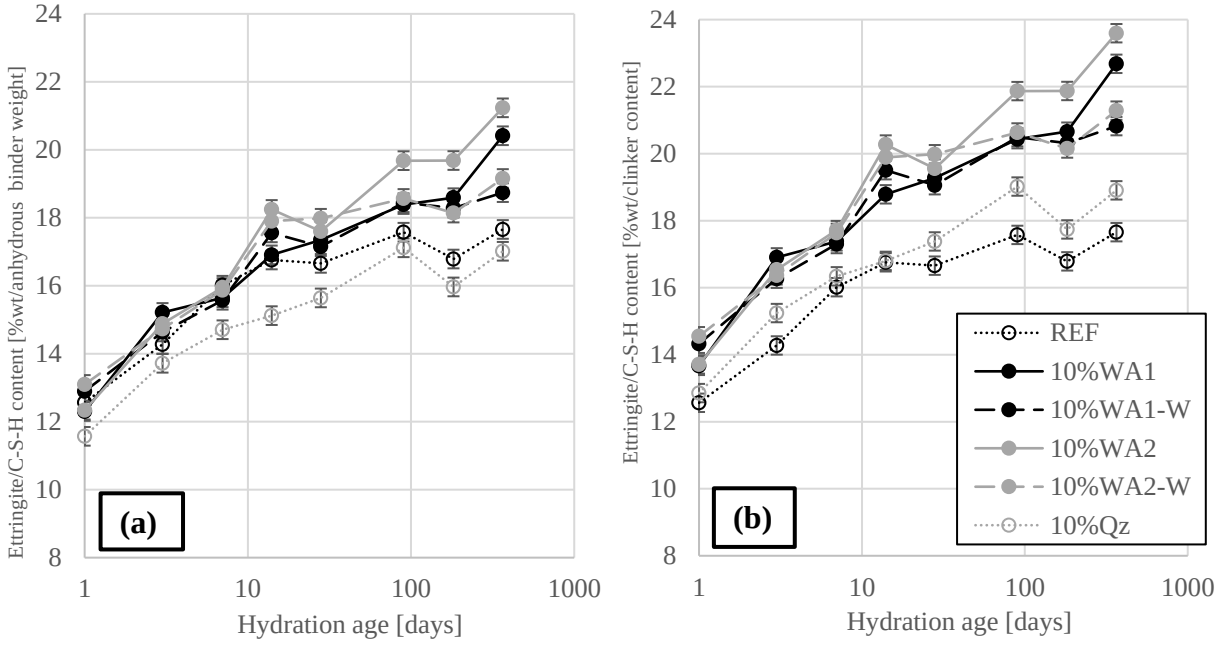

Figure 8. Quantification of ettringite/C-S-H in paste samples investigated after 1, 3, 7, 14, 28, 90, 182 and 365 days of hydration at 20°C. The results are normalised to the anhydrous binder (a) and clinker content (b). Standard deviations are based on three independent measurements and quantifications of the ettringite of a control sample at 28 days of hydration.

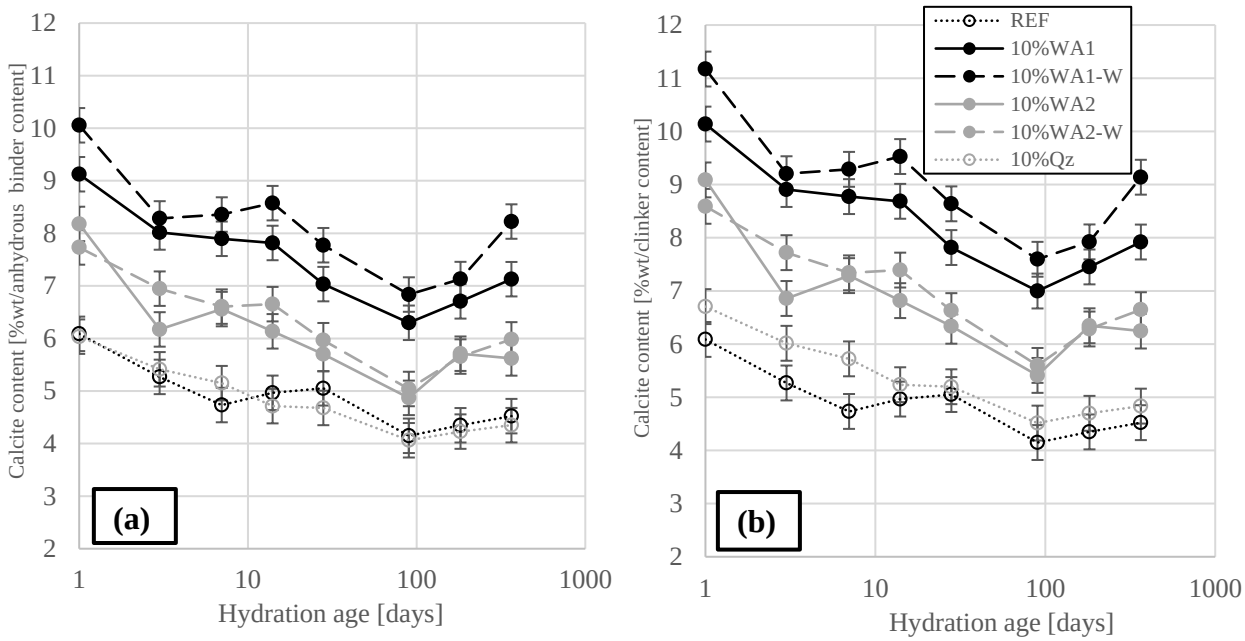

Figure 9. Quantification of calcite in paste samples investigated after 1, 3, 7, 14, 28, 90, 182 and 365 days of hydration at 20°C. The results are normalised to the anhydrous binder (a) and clinker content (b). Standard deviations are based on three independent measurements and quantifications of the calcite of a control sample at 28 days of hydration.